OXIDATION RESISTANCE OF LOW CARBON STAINLESS STEEL FOR APPLICATIONS IN SOLID OXIDE FUEL CELLS

M. Ziomek-Moroz, B. S. Covino, Jr., G. R. Holcomb, S. D. Cramer, S.J. Bullard,
S. A. Matthes, J. S. Dunning, D. E. Alman
U.S. Department of Energy, Albany Research Center, Albany, OR

Prabhakar Singh
Pacific Northwest National Laboratory, Richland, WA

Abstract

Alloys protected from corrosion by Cr_2O_3 (chromia) are recognized as potential replacements for $LaCrO_3$ –based ceramic materials currently used as bipolar separators (interconnects) in solid oxide fuel cells (SOFC). Stainless steels gain their corrosion resistance from the formation of chromia, when exposed to oxygen at elevated temperatures. Materials for interconnect applications must form uniform conductive oxide scales at 600–800° C while simultaneously exposed to air on the cathode side and mixtures of H_2 - H_2O, and, possibly, CH_x and CO - CO_2 on the anode side. In addition, they must possess good physical, mechanical, and thermal properties. Type 316L stainless steel was selected for the baseline study and development of an understanding of corrosion processes in complex gas environments.

This paper discusses the oxidation resistance of 316L stainless steel exposed to dual SOFC environment for ~100 hours at ~900°K. The dual environment consisted of dry air on the cathode side of the specimen and a mixture of H_2 and 3% H_2O on the anode side. Post - corrosion surface evaluation involved the use of optical and scanning electron microscopy and x-ray diffraction analyses.

Keywords: solid oxide fuel cell; dual environment; corrosion

INTODUCTION

Fuel cells are an emerging power generation technology that produce electricity and heat by electrochemically combining a gaseous fuel and oxidizing gas via an ion-conducting electrolyte [1]. The gaseous fuel could be in the form of pure hydrogen or reformed methane and the oxidizing gas could be in the form of pure oxygen or air. In solid oxide fuel cells (SOFCs), oxygen ions O^{2-} formed during the reduction reaction at the cathode side are moving through an ion-conducting electrolyte to the anode side to participate in the oxidation reaction along with hydrogen to form water. During the oxidation reaction, electrons are released and used in an outer circuit. : An example of a SOFC is shown in Figure 1.
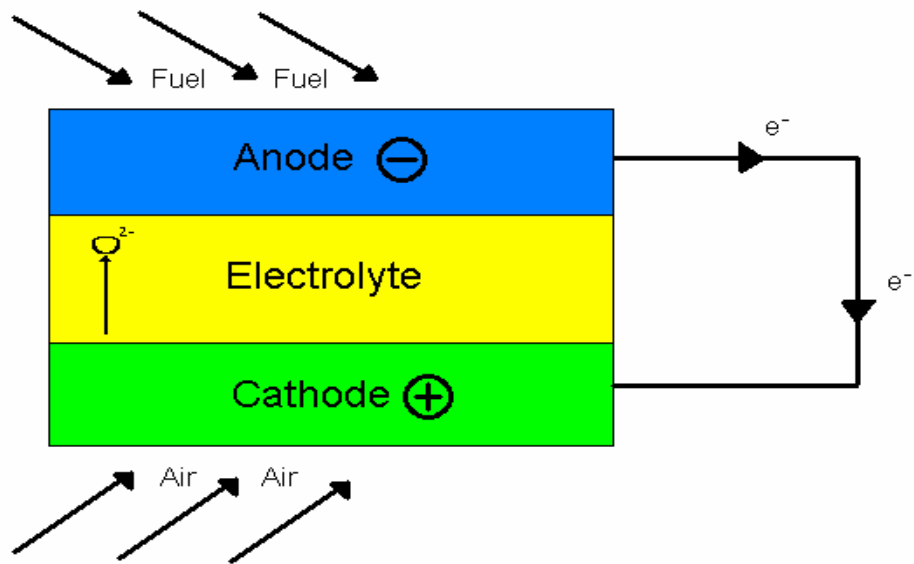
Fig. 1. Schematic diagram of single unit of solid oxide fuel cell showing generation of useful power.

The open circuit voltage of this type of the cell is approximately 1 V. To generate higher voltage, these cells are connected through a conductive interconnect or a bipolar separator as shown in Figure 2.
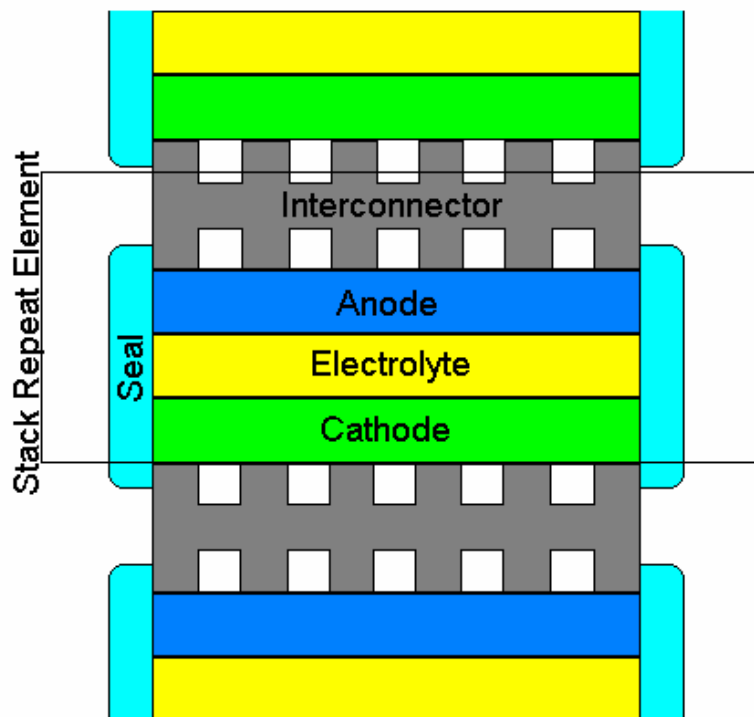

Fig. 2. Schematic diagram of sold oxide fuel cell stack.

The interconnect serves as a gas separator to prevent mixing of the fuel and air and provides electrical connection between individual cells. Therefore, it must exhibit good environmental stability in this dual reducing - oxidizing environment and have good electrical conductivity. For example, the formation of any insulating corrosion scale at the interface between interconnect cathode and/or anode membrane will adversary affect electrical conductivity of the interconnect.

Cost remains one of the major obstacles that must be overcome for fuel cells to realize their potential [6]. Cost reduction can be achieved in component fabrication, materials used, and cell and stack design. Replacing currently used ceramic interconnect materials with metallic interconnects can significantly reduce materials costs. Among the commercially available metallic materials, chromia (Cr_2O_3) scale-forming alloys appear to be the most promising candidates since they fulfill the technical and/or economical requirements [7]. Although chromia is not stable in the presence of oxygen and water vapor, 316L was selected for this base line study to develop of an understanding of corrosion processes occurring during simultaneous exposure of one side of the specimen to hydrogen and water vapor and the other side to air at ~900 ^{o}K.

EXPERIMENTAL PROCEDURES

Experiments were performed on commercial 316 stainless steel tubular specimens. The experiments were performed on the materials as received. The experimental setup is shown in Figure 3.
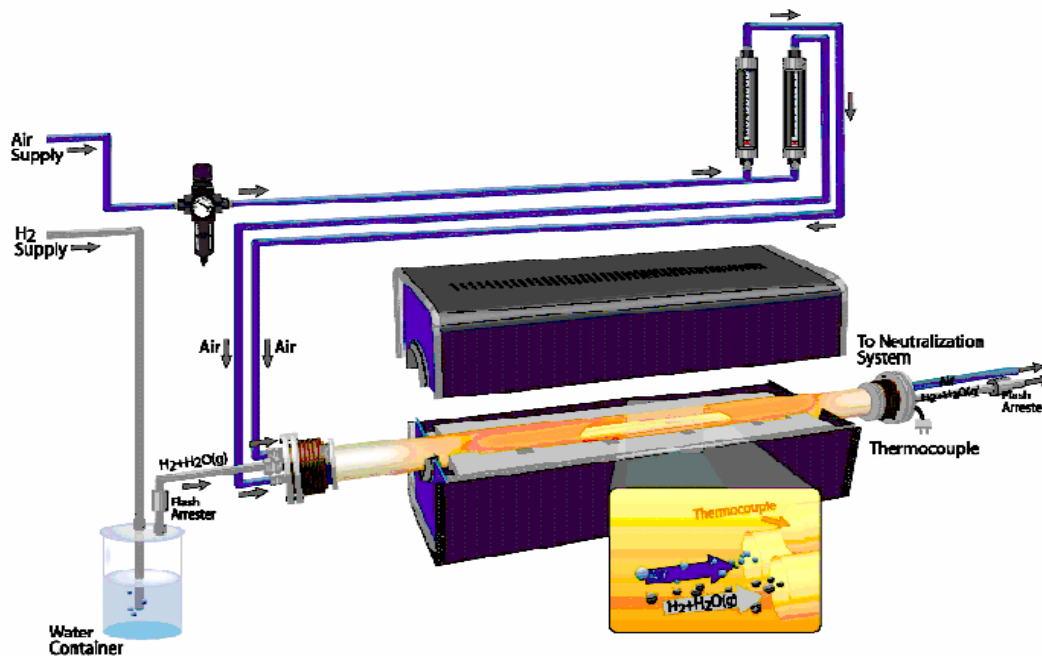

Fig. 3. Schematic diagram of experimental setup.

Two tubular specimens were inserted into a furnace. One specimen was exposed to a dual environment, e.g., the inner surface of the specimens was exposed to a mixture of H_2 and 3% H_2O while the outer surface to air. These experimental conditions are called a reducing/oxidizing environment. The other specimen was exposed to a singular environment, e.g., the inner and outer surfaces were exposed to air. These experimental conditions are called an oxidizing/oxidizing environment. The latter served as a control specimen. The experiment was carried out for 96 h at 907° K.

After the experiment, the specimen surfaces were observed using scanning electron microscopy (SEM) to determine surface microstructure. The chemical distribution of different elements in the corrosion products adhered to the surface was determined using energy dispersive X-ray (EDX) analysis mapping and wavelength dispersive X-ray (WDX) mapping. Also, crystalline oxides present in the scale removed from the specimen surface exposed to the air in the reducing/oxidizing environment were identified using X-ray diffraction (XRD).

RESULTS AND DISCUSSION

Oxidizing / oxidizing Environment

The SEM micrograph of the outer surface exposed to the air is shown in Fig. 4. As can be seen, the scale formed uniformly on the surface. Similar scale morphology was observed on 304 stainless steel in the oxidizing/oxidizing environment [8].
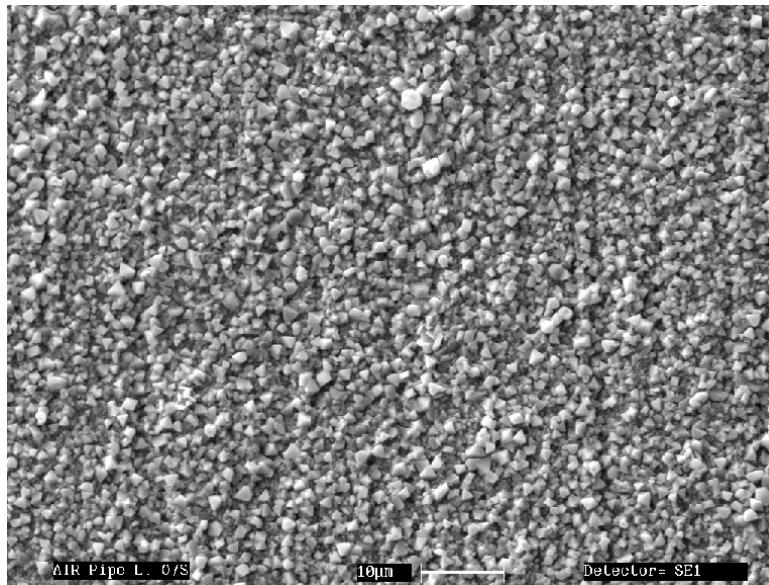

Fig. 4. SEM micrograph of tubular specimen outer surface exposed to air from oxidizing/oxidizing environment.

The WDX maps of the corrosion products reveal the presence of iron, chromium, and oxygen uniformly distributed on the surface as shown in Fig. 5.
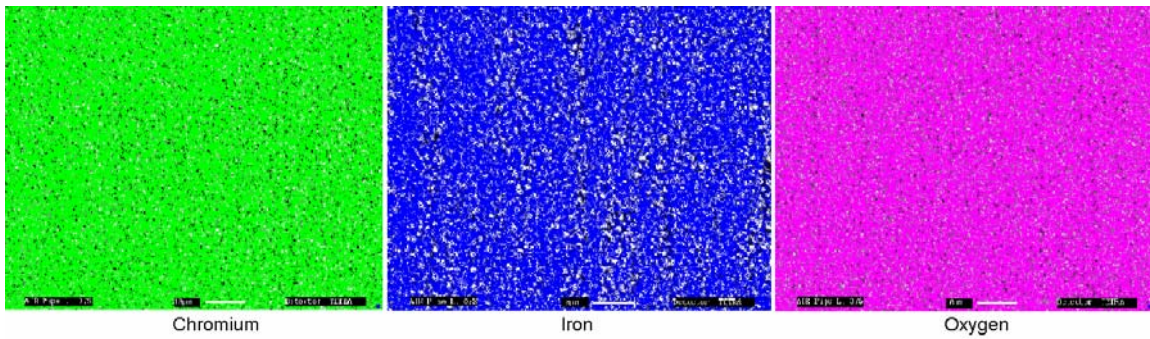

Fig. 5. WDX maps of chromium, iron, and oxygen for tubular specimen outer surface exposed to air from oxidizing/oxidizing environment.

The literature data indicate the formation of chromium oxide rich scale formed on 304 in the similar environment [8].

Also, a uniform scale was formed on the inner surface, Fig. 6.
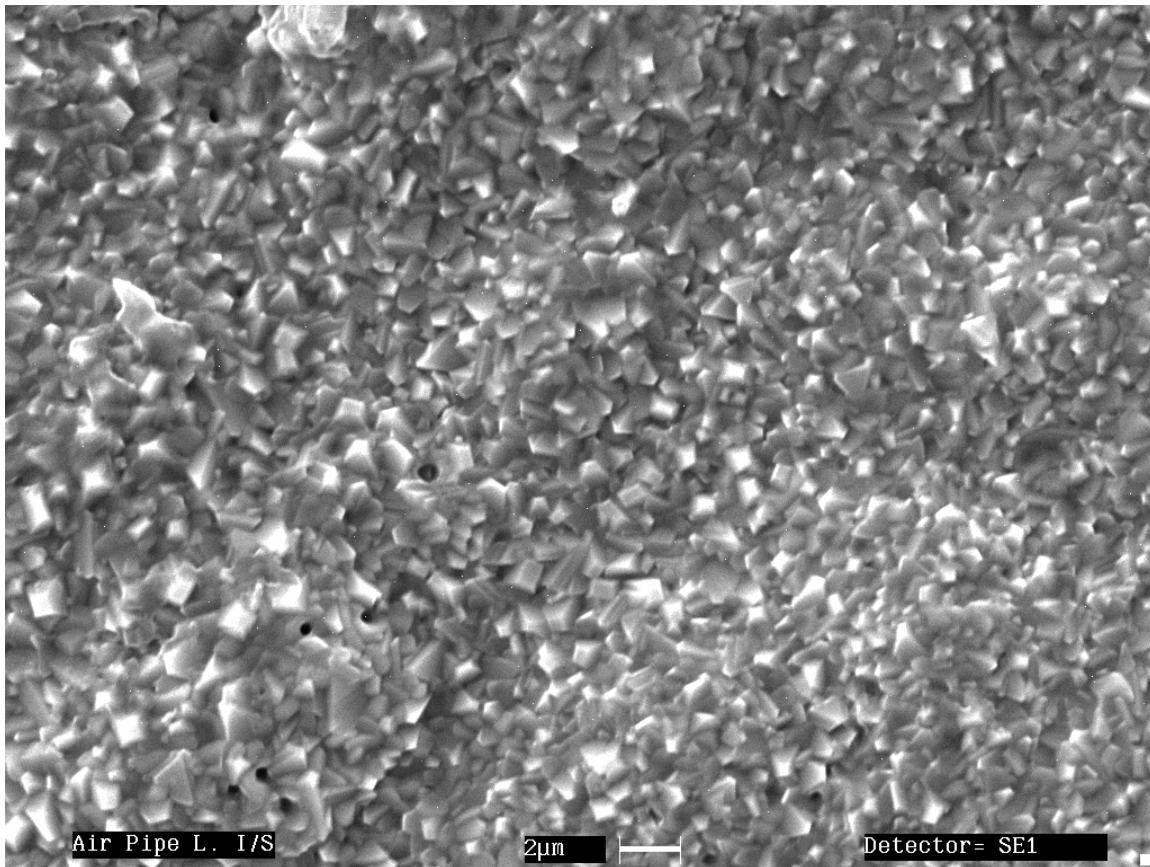

Fig. 6. SEM micrograph of tubular specimen inner surface exposed to air from oxidizing/oxidizing environment.

The EDX and WDX maps show the presence of chromium, iron, and oxygen on the surface. Higher concentration of chromium is observed in the groves as shown in Fig. 7.

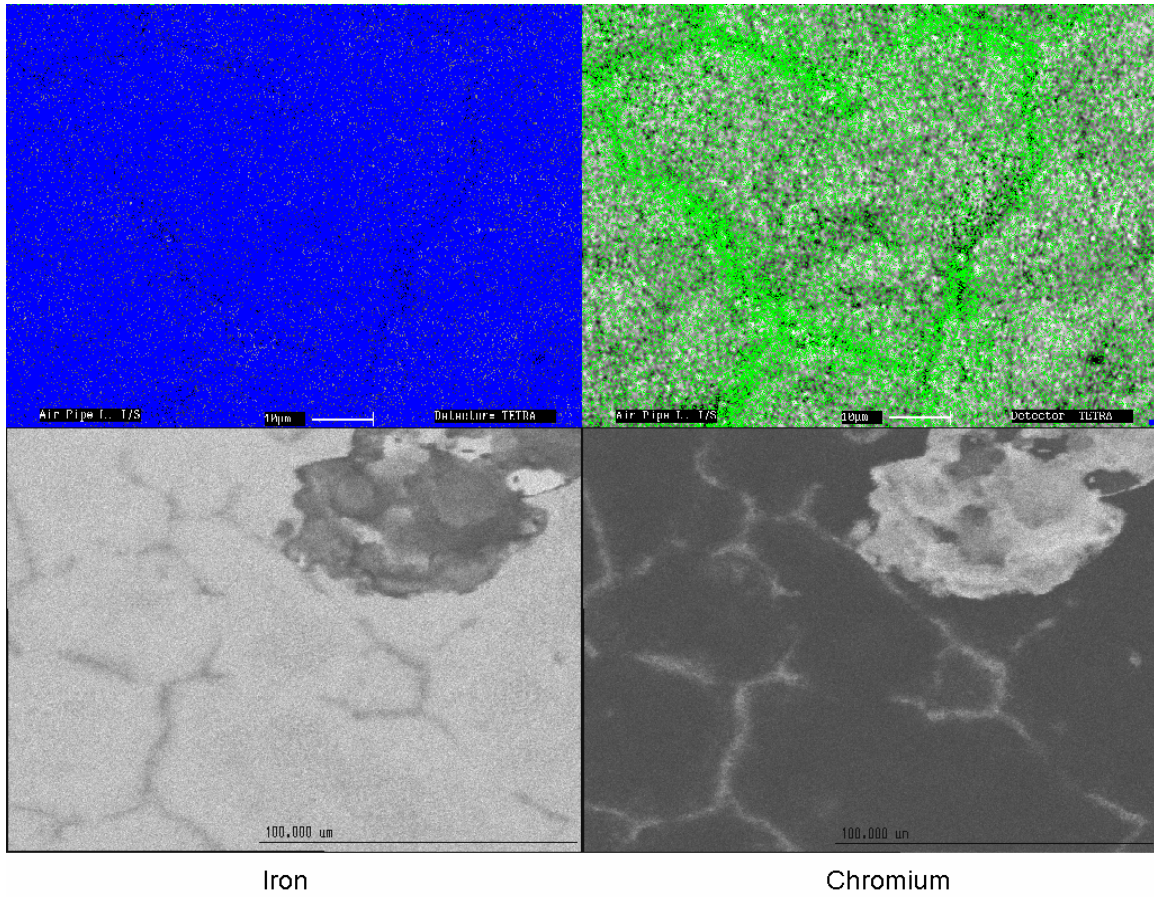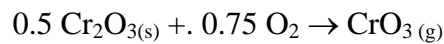Iron   Chromium

Fig. 7. WDX (top) and EDX (bottom) maps of chromium and iron for tubular specimen inner outer surface exposed to air from oxidizing/oxidizing environment. The presence of the groves resulted from the manufacturing process of the tubular specimens.

Reducing/ oxidizing Environment

In this dual reducing/oxidizing environment, corrosion stability of the investigated material is quite different from that in the oxidizing/oxidizing environment. The scale formed in the air, which simulates the cathode environment, is porous and flaky as shown in Figure 8.

The results of the (XRD) analysis of the scale removed from this surface indicate that the scale consists mainly of hematite Fe_2O_3 and traces of magnetite F_3O_4. The EDX and WDX elemental mapping of the scale adhered to the surface revealed the co-existence Cr and Fe oxides. The XRD, EDX, and WDX results may indicate a sandwich structure of the scale formed. The literature data indicate formation of the $Fe_2O_3/Fe_3O_4/Cr_2O_3/Fe_{(2-x)}Cr_xO_4$ sandwich structure for Fe-16Cr alloy oxidized at 1273° K, which may support our result [9]. Also, the lack of Cr_2O_3 in the scale outer layer can be due to evaporation of Cr_2O_3 according to the following reaction [10]:

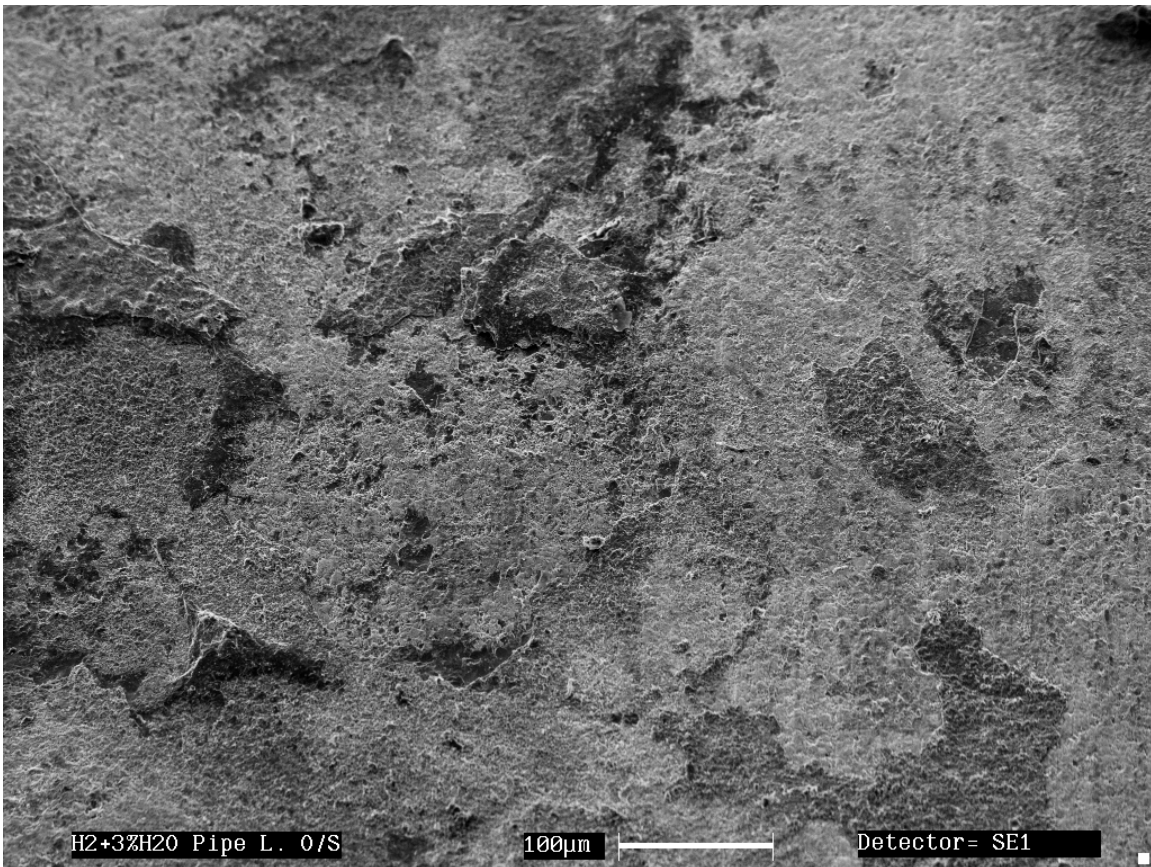$$0.5 \, Cr_2O_{3(s)} +. \, 0.75 \, O_2 \rightarrow CrO_{3 \, (g)}$$

Fig. 8. SEM micrograph of tubular specimen outer surface exposed to air from reducing/oxidizing environment.

In the simulated fuel environment, a non-continuous scale forms on the specimen surface as shown in Figure 9.
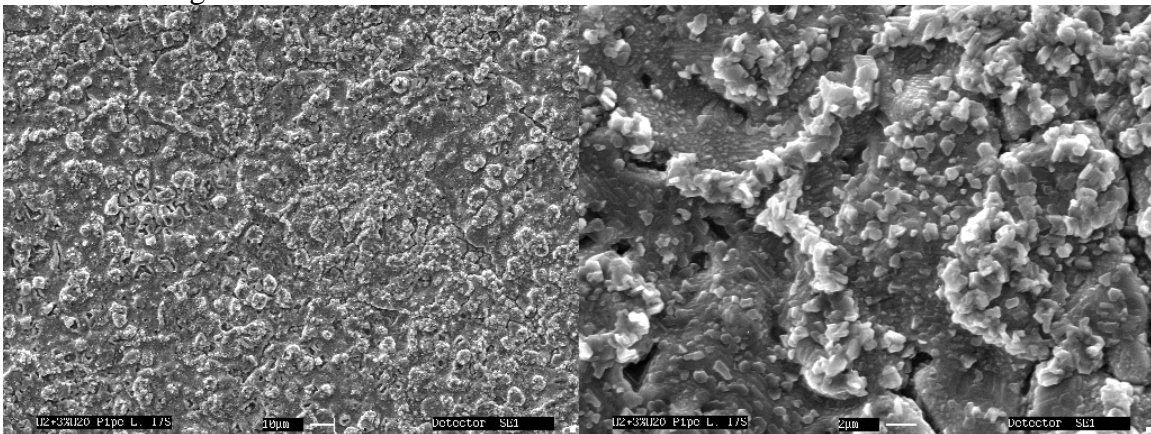

Fig. 9. SEM micrographs of tubular specimen inner surface exposed to $H_2 + 3\%H_2O$ from reducing/oxidizing environment at lower and higher magnification.

The EDX maps revealed the presence of chromium and iron oxides, Figure 10.
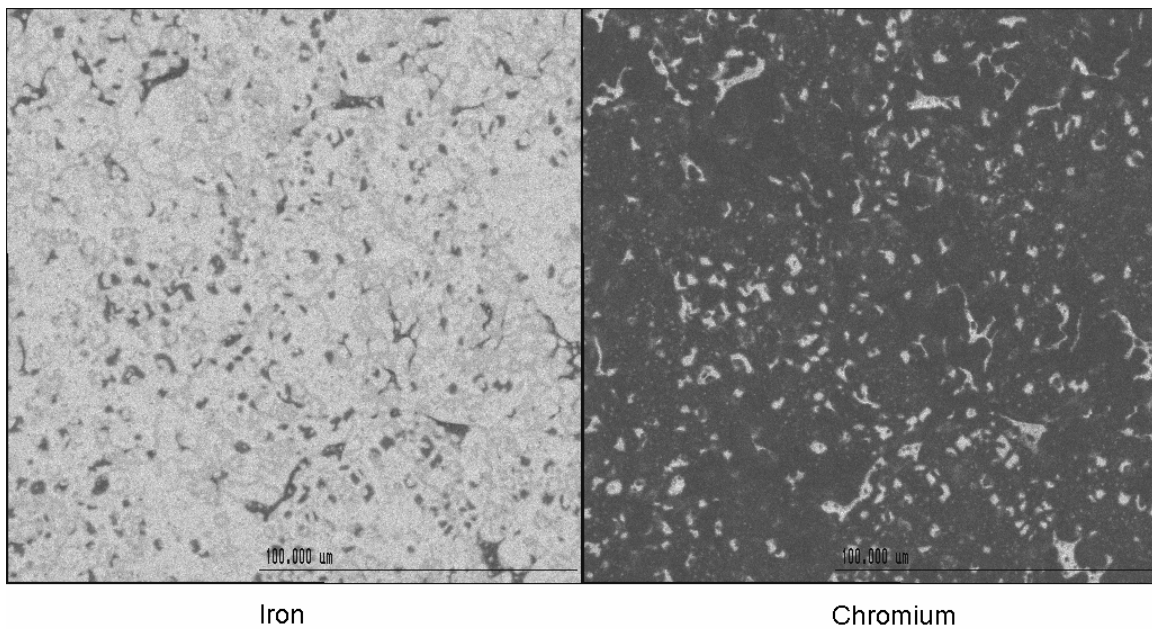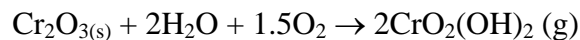
Iron   Chromium

Fig. 10. EDX maps of iron and chromium for tubular specimen inner outer surface exposed to $H_2 + 3\%H_2O$ from reducing/oxidizing environment.

Also, the maps show more iron than chromium in the scale. Lower concentration of chromium oxide could be associated with evaporation of chrome in the presence of water vapor according with the following reaction:

$$Cr_2O_{3(s)} + 2H_2O + 1.5O_2 \rightarrow 2CrO_2(OH)_2 \text{ (g)}$$

The literature data indicate that chromium oxyhydroxide is a predominant gaseous compound formed during evaporation, especially at low temperatures [8].

CONCLUSIONS

1. The SEM investigations of the surface exposed simultaneous to air on one side and air on the other side (oxidizing/oxidizing environment), reveal formation of uniform scales on both sides.

2. Elemental maps obtained by the WDX and EDX analyses indicate that the scale is enriched in chromium oxide, which is in good agreement with literature data.

3. The SEM investigations of the surface exposed simultaneous to the air on one side (oxidizing environment) and hydrogen + 3% water vapor on the other side show formation of porous and flaky scale in the oxidizing environment and non-continuous scale in the reducing environment.

4. The XRD, WDX, and EDX analyses of the corrosion products formed on 316 in the $H_2+3\%H_2O$ mixture revealed formation of iron oxide – rich scale with some chromium oxide. The presence of mostly iron oxide in the scale for this chromia-forming alloy indicates possible decomposition of chromium oxide in contact with H_2O.

5. The corrosion behavior of 316 in the singular oxidizing/oxidizing environment is different from the corrosion behavior in the dual oxidizing/reducing environment. This indicates that close simulation of industrial conditions in the laboratory is of utmost importance in corrosion studies of materials for their applications in SOFC stack and balance of plant (BOP).

ACKNOWLEDGEMENTS

REFRENCES

1. Fuel Cell Handbook, fifth edition, U.S. Department of Energy, Office of Fossil Energy, National Energy Technology Laboratory

2. Nguyen Q. Minh, J. Am. Ceram. Soc., 76 (3) 563-88 (1993)

3. W.A. Meulenberg, S. Uhlenbruck, E. Wessel, H. P. Buchkremer, D. Stöver, J. Mat. Sci., 38 , 507-513, (2003)

4. P. Singh, L. R. Pederson, S.P. Simner, J. W. Stevenson, V. V. Viswanathan "Solid Oxide Fuel Cell Power Generation Systems," Proceedings of IECEC: 36th Annual Intersociety Energy Conversion Engineering Conference Advance Program

5. Diane England, Private Communication

6. SECA Program Plan – Making Fuel Cells Available to America, U.S. Department of Energy, National Energy Technology Laboratory, Pacific Northwest National Laboratory

7. Z.G. Yang, K.S. Weil, D.M. Paxton, and J.W. Stevenson, 2002 Fuel Cell Seminar Abstracts, p. 522

8. Prabhakar Singh & Z. Gary Yang, Thermo chemical analysis of Oxidation and Corrosion Processes in High Temperature Fuel Cells, Presented at 131st TMS Annual Meeting. Seattle, WA. February 18, 2002

9. D. A. Jones, Principles and Prevention of Corrosion, Prentice Hall, Inc., 1996

10. H. L. Tuller, Electroceramics – Materials, Processing and Characterization: Application to Solid Oxide Fuel Cells, NETL Workshop, Morgantown, WV, June 16-17, 2003